

## RESEARCH ARTICLE



# IDH2-NADPH pathway protects against acute pancreatitis via suppressing acinar cell ferroptosis

Qi Peng<sup>1,2</sup> | Bin Li<sup>1,2</sup> | Pengli Song<sup>1,2</sup> | Ruiyan Wang<sup>1,2</sup> | Jing Jiang<sup>1,2</sup> |  
Xuerui Jin<sup>1,2</sup> | Jie Shen<sup>1,2</sup> | Jingpiao Bao<sup>1,2</sup> | Jianbo Ni<sup>1,2</sup> | Xiao Han<sup>1,2</sup> |  
Guoyong Hu<sup>1,2</sup>

<sup>1</sup>Department of Gastroenterology, Shanghai General Hospital, Shanghai, China

<sup>2</sup>Shanghai Key Laboratory of Pancreatic Disease, Institute of Pancreatic Disease, Shanghai Jiao Tong University School of Medicine, Shanghai, China

## Correspondence

Guoyong Hu, Xiao Han, and Jianbo Ni,  
Department of Gastroenterology and Shanghai  
Key Laboratory of Pancreatic Disease,  
Shanghai General Hospital, Shanghai Jiao Tong  
University School of Medicine, 100 Haining  
Road, Shanghai 200080, China.  
Email: [huguoyongsh@sina.com](mailto:huguoyongsh@sina.com);  
[hanxiao714@126.com](mailto:hanxiao714@126.com) and [jianbo.ni@shgh.cn](mailto:jianbo.ni@shgh.cn)

## Funding information

National Natural Science Foundation of China,  
Grant/Award Numbers: 81970556,  
8217031247, 82200716

## Abstract

**Background and Purpose:** Acute pancreatitis (AP) is associated with acinar cell death and inflammatory responses. Ferroptosis is characterized by an overwhelming lipid peroxidation downstream of metabolic dysfunction, in which NADPH-related redox systems have been recognized as the mainstay in ferroptosis control. Nevertheless, it remains unknown how ferroptosis is regulated in AP and whether we can target it to restrict AP development.

**Experimental Approach:** Metabolomics were applied to explore changes in metabolic pathways in pancreatic acinar cells (PACs) in AP. Using wild-type and *Ptf1a*<sup>CreERT2/+IDH2<sup>fl/fl</sup> mice, AP was induced by caerulein and sodium taurocholate (NaT). IDH2 overexpressing adenovirus was constructed for infection of PACs. Mice or PACs were pretreated with inhibitors of FSP1 or glutathione reductase. Pancreatitis severity, acinar cell injury, mitochondrial morphological changes and pancreatic lipid peroxidation were analysed.</sup>

**Key Results:** Unsaturated fatty acid biosynthesis and the tricarboxylic acid cycle pathways were significantly altered in PACs during AP. Inhibition of ferroptosis reduced mitochondrial damage, lipid peroxidation and the severity of AP. During AP, the NADPH abundance and IDH2 expression were decreased. Acinar cell-specific deletion of IDH2 exacerbated acinar cell ferroptosis and pancreatic injury. Pharmacological inhibition of NADPH-dependent GSH/GPX4 and FSP1/CoQ<sub>10</sub> pathways abolished the protective effect of IDH2 overexpression on ferroptosis in acinar cells. CoQ<sub>10</sub> supplementation attenuated experimental pancreatitis via inhibiting acinar cell ferroptosis.

**Conclusion and Implications:** We identified the IDH2-NADPH pathway as a novel regulator in protecting against AP via restricting acinar cell ferroptosis. Targeting the pathway and its downstream may shed light on AP treatment.

**Abbreviations:** AGI, AGI-6780; AP, acute pancreatitis; ASCL4, acyl-coA synthetase long chain family member 4; Cae, caerulein; CoQ<sub>10</sub>, coenzyme Q<sub>10</sub>; DFO, deferoxamine mesylate; Fer-1, Ferrostatin-1; FSP1, ferroptosis suppressor protein 1; GPX4, glutathione peroxidase 4; GR, glutathione reductase; GSH, glutathione; GSSG, oxidized glutathione; H&E, haematoxylin-eosin; hetKO, heterozygous knockout; IDH2, isocitrate dehydrogenase 2; MDA, malondialdehyde; ME, malic enzyme; NADH, nicotinamide adenine dinucleotide; NADK, NAD kinase; NADPH, nicotinamide adenine dinucleotide phosphate; NaT, sodium taurocholate; NOX, NADPH oxidase; OPLS-DA, orthogonal partial least squares discriminant analysis; PACs, pancreatic acinar cells; PCA, principal component analysis; PI, propidium iodide; PPP, pentose phosphate; PUFAs, polyunsaturated fatty acids; TCA, tricarboxylic acid; UPLC-MS/MS, ultra-high-performance liquid chromatography tandem mass spectrometry; WT, wild-type;  $\alpha$ -KG,  $\alpha$ -ketoglutarate.

Qi Peng, Bin Li and Pengli Song contributed equally to this work.

## KEYWORDS

acute pancreatitis, ferroptosis, isocitrate dehydrogenase 2, nicotinamide adenine dinucleotide phosphate

## 1 | INTRODUCTION

Acute pancreatitis (AP) is one of the most common gastrointestinal conditions with substantial morbidity and hospital admissions. As a complex disease with a variable course, AP can progress towards severe disease in approximately one fifth of patients, resulting in a mortality rate of around 20% (Mederos et al., 2021). Therefore, there is an urgent need for further exploration of the exact pathological cellular pathways underlying AP. Hallmarks of AP are well recognized as acinar cell death and inflammatory responses, and pancreatic necrosis determines the severity of AP and patient mortality (Lee & Papachristou, 2019; Wang et al., 2016). However, the pathogenesis of AP involves multiple distinct cell death pathways, and the molecular mechanism of acinar cell necrosis has not been fully elucidated.

Ferroptosis is a form of programmed cell death and has gained significant attention for its potential to inhibit tumour cells, while recent research has suggested that ferroptosis may be involved in the development of AP (Dixon et al., 2012; Ma et al., 2021). During AP, blocking ferroptosis using specific inhibitors or antioxidants can alleviate pancreatic damage as well as systemic organ failure including liver, lung and kidney injury (Fan et al., 2021; Ma et al., 2021; Y. Zheng et al., 2022). While several ferroptosis-related genes and pathways have been identified in AP, the specific regulatory mechanisms remain poorly understood.

Ferroptosis is induced by iron-dependent accumulation of lipid peroxides, which is closely associated with iron, amino acid and lipid metabolism (Dixon et al., 2012; Tang et al., 2021). The **glutathione** (GSH)/**glutathione peroxidase 4** (GPX4) axis and ferroptosis suppressor protein 1 (FSP1)/coenzyme Q<sub>10</sub> (CoQ<sub>10</sub>) axis have been identified as the major independent inhibitory pathways of ferroptosis, which modulate the clearance of lipid peroxides (Doll et al., 2019; Friedmann Angeli et al., 2014). Of these, nicotinamide adenine dinucleotide phosphate (**NADPH**) acts as a reducing equivalent to catalyse the recycling of reduced GSH, thereby assisting GPX4 in scavenging lipid peroxides (Ursini & Maiorino, 2020). Additionally, FSP1 promotes the regeneration of reduced CoQ<sub>10</sub> in a NADPH-dependent manner and regulates ferroptosis (Bersuker et al., 2019). In fact, NADPH has been recognized as a marker of ferroptosis sensitivity in several cancer cell lineages, and NADPH phosphatase, MESH1, sensitizes cells to ferroptosis by depleting NADPH (Ding et al., 2020; Shimada et al., 2016).

In this study, we investigated the role and the associated mechanisms of ferroptosis in AP. **Isocitrate dehydrogenase 2** (IDH2), a key enzyme of the tricarboxylic acid (TCA) cycle, was identified as an inhibitory molecule of ferroptosis in AP. Acinar cell-specific IDH2 deficiency facilitated acinar cell ferroptosis and exacerbated AP. Mechanically, IDH2 attenuated acinar cell ferroptosis by enhancing NADPH-dependent GSH/GPX4 and FSP1/CoQ<sub>10</sub> pathways, and thereby alleviated experimental pancreatitis. These findings establish

### What is already known

- Ferroptosis may be involved in the development of various diseases, including acute pancreatitis.
- NADPH can be associated with ferroptosis sensitivity in some diseases.

### What does this study add

- Mitochondrial IDH2 protects against acinar cell ferroptosis through enhancing NADPH-dependent GSH/GPX4 and FSP1/CoQ<sub>10</sub> pathways.
- CoQ<sub>10</sub> supplementation attenuates experimental pancreatitis via inhibiting acinar cell ferroptosis.

### What is the clinical significance

- Targeting the IDH2-NADPH pathway and its downstream may shed new light on AP treatment.

ferroptosis as essential mediators of acinar cell death during AP, and identify NADPH-related pathways as potentially novel targets for treatment of AP.

## 2 | METHODS

### 2.1 | Animal models

Wild-type (WT) C57BL/6J mice (RRID:IMSR\_JAX:000664, 6–8 weeks, 20–22 g, male) were purchased from Shanghai SLAC Laboratory Animal Co Ltd. IDH2<sup>fl/fl</sup> mice (RRID:IMSR\_NM-CKO-205094) were purchased from Shanghai Model Organisms Center, Inc. Ptf1a<sup>CreERT2</sup> mice (RRID:IMSR\_NM-KI-200118) were kindly gifted by Professor Jing Xue from Institute of State Key Laboratory of Oncogenes and Related Genes, Stem Cell Research Center, Ren Ji Hospital, Shanghai Jiao Tong University School of Medicine, Shanghai, China. To generate mice with acinar cell-specific deletion of IDH2 (Ptf1a<sup>CreERT2/+</sup>IDH2<sup>fl/fl</sup>), IDH2<sup>fl/fl</sup> mice were crossed with Ptf1a<sup>CreERT2/+</sup> mice. All mice (20–22 g, male) were ear tagged and randomized into groups using a completely randomized table (n = 5 per group). All mice were housed under a controlled environment in individually ventilated cages with wood

shavings as bedding (four to six mice per cage), 12-h dark/light cycle at 22°C and free access to water and standard rodent chow. All animal experiments were conducted according to the replacement, refinement and reduction (3Rs) principle; and in accordance with animal welfare legislation and were approved by the Animal Ethics Committee of Shanghai General Hospital (2019-A053-02). Animal studies were conducted in accordance with the ARRIVE guidelines (Percie du Sert et al., 2020) and the recommendations of the *British Journal of Pharmacology* (Lilley et al., 2020).

## 2.2 | Induction of experimental pancreatitis and treatments

Caerulein-induced AP was induced in mice by administering 10 hourly intraperitoneal injections of caerulein ( $100 \mu\text{g}\cdot\text{kg}^{-1}$ ); humane killing was performed 12 h after the first injection (Hu et al., 2011). Mice were killed by cervical dislocation after inducing anaesthesia with 3% isoflurane. Sodium taurocholate-induced AP was induced as follows. Mice were anaesthetised using 3% isoflurane. Following shaving, a 2–3 mm incision was made in the abdomen and part of the duodenum was gently removed with forceps. The duodenal papilla region was exposed, and the common bile duct was closed with vascular clips. Using a stereomicroscope, a blunt-tipped puncture needle was used to puncture the pancreatic duct and the end of the puncture needle was connected to a micro-infusion pump for retrograde pancreaticobiliary injection, and 2.5% sodium taurocholate solution ( $2 \text{ mg}\cdot\text{kg}^{-1}$ ) was slowly infused at a rate of  $5 \mu\text{l}/\text{min}$ , or an equal volume of saline in the control group. After completing the infusion process, the vascular clips were carefully removed, the puncture needles and clips were withdrawn, and the organs were gently reset into the abdominal cavity, and the wound was closed with 6/0 surgical sutures. Mice were placed on a 37°C heating pad until recovery. Humane killing was performed 24 h after surgery (Perides et al., 2010). After surgery, the mice were returned to their cages placed on a heated pad (37°C) until they recover. Mice injected with an equal volume of saline served as the control. Ferrosstatin-1 (Fer-1;  $5 \text{ mg}\cdot\text{kg}^{-1}$ ), deferoxamine mesylate (DFO;  $50 \text{ mg}\cdot\text{kg}^{-1}$ ), iFSP1 ( $1 \text{ mg}\cdot\text{kg}^{-1}$ ), 2-AAPA ( $10 \text{ mg}\cdot\text{kg}^{-1}$ ) and CoQ<sub>10</sub> ( $50 \text{ mg}\cdot\text{kg}^{-1}$ ) were administered intraperitoneally 1 h before the first injection of caerulein or retrograde injection of sodium taurocholate, respectively. The pathologists analysing the data were blinded to the experiment groups.

## 2.3 | Isolation of pancreatic acini and treatments

Mouse pancreatic acinar cells (PACs) were prepared by collagenase digestion procedure as previously described (B. Li et al., 2020; Wen et al., 2015), with minor modifications. Briefly, the pancreas was resected and washed with phosphate-buffered saline. Mouse pancreatic tissues were isolated and incubated at 37°C for 20 min after multipoint injection of 1 ml of collagenase IV ( $2 \text{ mg}\cdot\text{ml}^{-1}$ ; MP Biomedicals, CA, USA). The tissues were then separated by blowing repeatedly with wide bore pipette tips until the large pancreatic tissues

disappeared. The tissue was filtered through a 70- $\mu\text{m}$  cell strainer (Corning, NY · USA), centrifuged, washed and resuspended in DMEM/F-12 culture medium containing 10% fetal bovine serum. PACs were pretreated with iFSP1 ( $5 \mu\text{M}$ ) or AGI ( $10 \mu\text{M}$ ) for 1 h, or with 2-AAPA ( $25 \mu\text{M}$ ) for 0.5 h, followed by stimulation with NaT ( $4 \text{ mM}$ ). PACs were collected for further examination as described in the relevant figure legends.

## 2.4 | Histology and immunohistochemistry

The fresh pancreatic tissues were collected, fixed with 4% paraformaldehyde for 24 h, and sectioned into 4- $\mu\text{m}$  slices for haematoxylin–eosin (H&E) staining using routine procedures. Pancreatic injuries were scored from 0 to 3 for oedema, inflammation and necrosis in a blinded fashion by two experienced investigators (Wildi et al., 2007). For immunohistochemical staining, paraffin-embedded pancreatic sections were dewaxed, rehydrated and incubated with Citrate Antigen Retrieval Solution (Sangon Biotech, Shanghai, China). Sections were then incubated with monoclonal antibody against CD45 (1:100) or MDA (1:100) overnight, visualized using an immunohistochemistry kit (Vector Laboratories, Burlingame, USA).

## 2.5 | Immunofluorescence staining

Paraffin-embedded pancreatic sections were dewaxed, rehydrated and microwaved in Citrate Antigen Retrieval Solution (Sangon Biotechnology, Shanghai, China). Sections were then blocked for 1 h with 10% goat serum. Subsequently, they were incubated overnight with primary antibodies against amylase (1:100) and IDH2 (1:100). After being washed three times in PBS, sections were incubated with secondary antibodies (Alexa Fluor 594-conjugated goat anti-rabbit or FITC-conjugated goat anti-mouse; 1:100) for 1 h at 37°C. Nuclei were stained with DAPI for 10 min and all samples were mounted with fluorescent mounting medium (Yeaston Technology, Shanghai, China). Results of immunofluorescence staining were visualized and analysed using a Leica SP8 confocal microscope and LAS X software (RRID: SCR\_013673, Leica Application Suite X, Leica, IL, USA).

## 2.6 | Serum amylase and lipase assay

The serum was obtained by centrifugation at 1734 g for 15 min at 4°C. Serum amylase and lipase levels were measured by a Roche/Hitachi modular analytics system (Roche Diagnostics, Basel, Switzerland).

## 2.7 | PI uptake

When the acinar cell treatment reached the end point, the cells of each group were transferred to a new 96-well plate; 2  $\mu\text{l}$  of propidium

iodide (PI; 2.5 mg·ml<sup>-1</sup>; Sigma, Missouri, USA, cat#P4170) was added into each well and incubated at room temperature for 5 min. The first reading (Read 1) was performed on the microplate reader (Thermo Varioskan Flash, MA, USA) at Ex/Em = 536/617 nm. Next, 2 µl of 25% Triton-X100 (Sangon Biotech, cat#A110694) was added into each well, and the wells were incubated at room temperature for 20 min. The second reading (Read 2) was conducted on the microplate reader at Ex/Em = 536/617 nm. The PI uptake (%) can be calculated as the mean of Read 1/Read 2 × 100% for each group.

## 2.8 | Metabolomic analysis of PACs

The metabolites of PACs were quantified using an ultra-high-performance liquid chromatography tandem mass spectrometry (UPLC-MS/MS) system (ACQUITY UPLC-Xevo TQ-S, Waters Corp., Milford, MA, USA). The UPLC-MS/MS generated raw data files that were processed using TMBQ software (v1.0, Metabo-Profile, Shanghai, China) to perform peak integration, calibration and quantification for each metabolite. The iMAP platform (v1.0, Metabo-Profile, Shanghai, China), which was internally developed, was implemented to conduct statistical analyses, including principal component analysis (PCA), orthogonal partial least squares discriminant analysis (OPLS-DA), univariate, and pathway analyses.

## 2.9 | IDH2 adenovirus infection and acinar cell imaging

Primary acinar cells were plated at the appropriate density, and then  $1 \times 10^9$  PFU·ml<sup>-1</sup> IDH2 overexpression adenovirus or the control adenovirus (OBiO, Shanghai, China) was added to the culture medium. After 6 h of infection, the fluorescent protein expressed on the adenovirus plasmid was observed to determine the infection efficiency and replace with the fresh culture medium and cultured for 18 h for further processing. At the end of the experiment, the acinar cells were collected and the expression of IDH2 was measured to determine the effect of adenoviral intervention.

## 2.10 | Measurement of MDA

According to the instruction of the MDA assay kit (Sigma, cat#-MAK085), fresh pancreatic tissue (10 mg) or appropriate amount of PACs were homogenized on ice in 300 µl of the MDA Lysis Buffer containing 3 µl of BHT (100×). Centrifuge the samples at 13,000 g for 10 min to remove insoluble material. 100 µl of the supernatant from each homogenized sample was transferred into a microcentrifuge tube and 300 µl of TBA solution added. This was incubated at 95°C for 60 min and then cooled to room temperature in an ice bath for 10 min; 200 µl of the MDA-TBA adduct was extracted into a 96-well plate, and the concentration of MDA in each sample was calculated using a fluorescent microplate reader (Ex/Em = 532/553 nm).

## 2.11 | BODIPY 581/591 staining

At 30 min before the primary acinar cells reached the end point of treatment, BODIPY 581/591 C11 solution (5 µM; Invitrogen, cat#D3861) was added to the medium and incubated at 37°C for 30 min. The cells were collected, centrifuged to discard the supernatant and washed twice with PBS. Then the cells were fixed with 300 µl of 4% paraformaldehyde for 10 min at room temperature, and the fluorescence changes of each group were visualized and analysed using a Leica SP8 confocal microscope and LAS X software (Leica, IL, USA).

## 2.12 | Measurement of NADPH

According to the instruction of the NADP/NADPH Assay Kit (Amplite, CA, USA, cat#15264), take fresh pancreatic tissue (10 mg) or an appropriate amount of primary acinar cells and place them into 200 µl of NADP/NADPH lysis solution. After homogenization and centrifugation, 25 µl of the supernatant was removed into a 96-well plate. 25 µl of NADPH extraction solution was added and it was incubated at room temperature for 15 min. Then, 25 µl of NADP extraction solution was added and it was incubated at room temperature for 1 h. The concentration of NADPH in each sample was calculated by taking a reading from a fluorescence microplate reader (Ex/Em = 540/590 nm).

## 2.13 | Western blotting

Total protein isolated from pancreatic tissues and PACs were extracted using the method described previously (Hu et al., 2011). Proteins (40 µg per lane) were submitted to 10% or 12.5% SDS-PAGE (Epizyme Biotech, Shanghai, China) and electrotransferred to nitrocellulose membranes (Millipore, CA, USA). The membranes were then incubated overnight at 4°C with primary antibodies against GPX4 (1:1000), ACSL4 (1:1000), IDH2 (1:1000) and β-actin (1:800). Samples were then probed with secondary antibodies for 1 h at 37°C and visualized by an Odyssey CLx imaging system (LI-COR, Nebraska, USA). Densitometric analysis was performed using the Image Studio system and normalized to β-actin. Protein levels of experimental groups were represented as fold changes compared with the control group. The immuno-related procedures employed are in line with recommendations established by the *British Journal of Pharmacology* (Alexander et al., 2018).

## 2.14 | Real-time quantitative PCR (qRT-PCR)

Total RNA was isolated from pancreatic tissues and PACs using Trizol reagent (Invitrogen, CA, USA), and RNA concentration and purity were measured using a spectrophotometer (Thermo Scientific, MA, USA). Reverse transcription was performed using the PrimeScript RT reagent kit (Takara Bio, Inc, Kyoto, Japan). RT-qPCR was performed by SYBR Premix Ex Taq (Takara Bio, Inc) in the QuantStudio 6 Flex Real-Time PCR System (Applied Biosystems, CA, USA). Relative



expression of target genes and fold changes were calculated using the comparative CT ( $2^{-\Delta\Delta CT}$ ) method with Rplp0 as a reference gene. The mean values of the control group were set to 1, and the values of all other groups were normalized to the control group values, presented

as the fold mean of the controls. Each target gene was analysed with three replicates for each biological sample, and at least five biological samples were analysed in each condition. Primers (Sangon Biotechnology) for RT-PCR experiments are listed in Table S1.

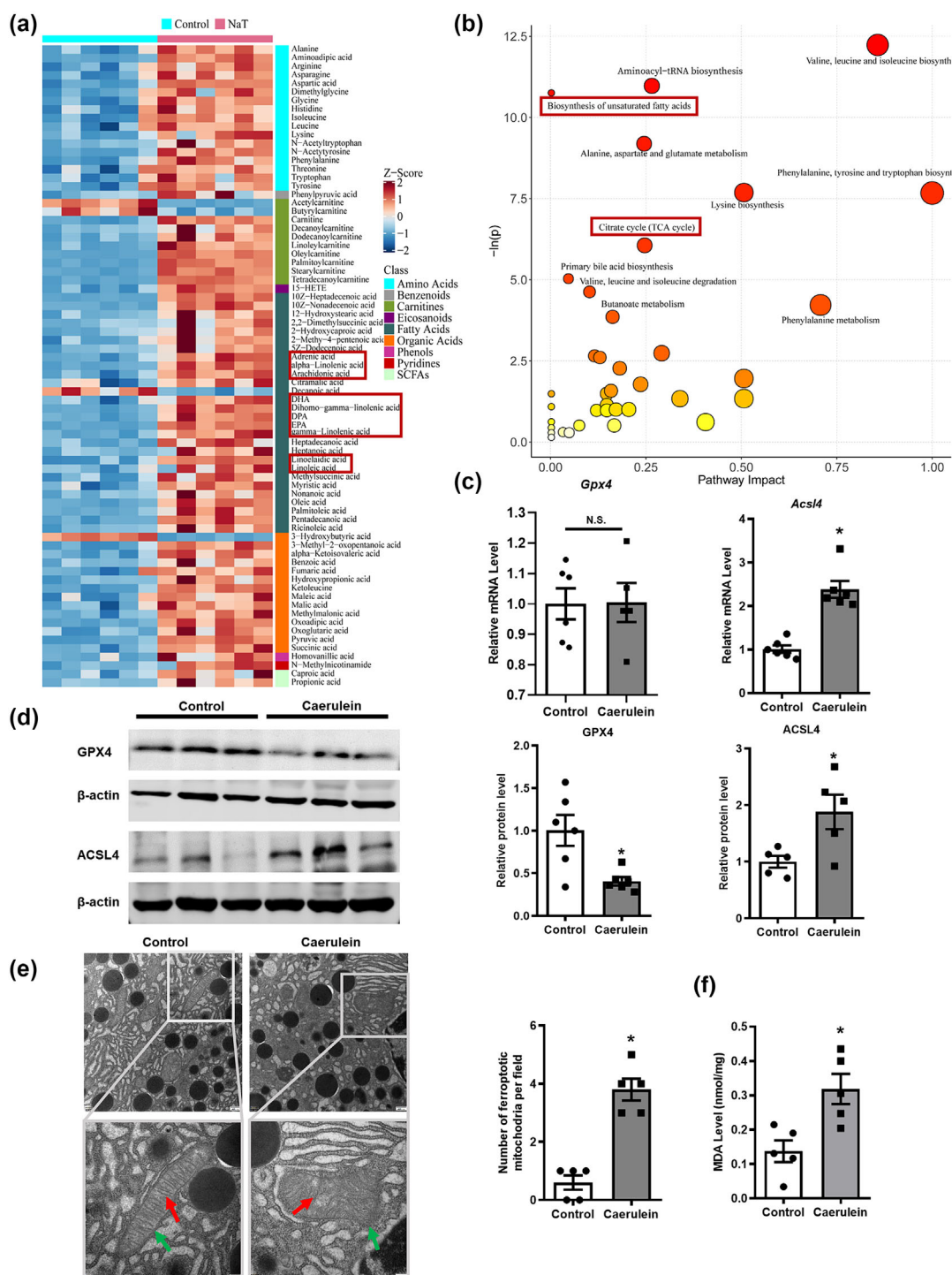


**FIGURE 1** Ferroptosis of acinar cells is present in acute pancreatitis (AP). In vivo, AP was induced by injections of caerulein (Cae, 100  $\mu\text{g}\cdot\text{kg}^{-1}$ ). In vitro, freshly isolated pancreatic acinar cells (PACs) were stimulated with 4-mM sodium taurocholate (NaT) for 1 h. (a,b) Significant changes in unsaturated fatty acid metabolic pathways and the tricarboxylic acid cycle in PACs stimulated by NaT. qRT-PCR (c) and immunoblot analysis (d) of GPX4 and ACSL4 expression in pancreatic tissue. (e) Mitochondrial morphological changes in the acinar cells in response to caerulein at low power (scale bar = 500 nm) and high power (scale bar = 200 nm). Five representative fields of view were selected for each group. (f) Pancreatic level of MDA in mice with control or AP.  $n = 5$  per group. Data are shown as mean  $\pm$  SEM. \* $P < 0.05$  versus control, N.S. = not significant.

## 2.15 | Transmission electron microscopy

Fresh pancreatic tissue (about 1 mm<sup>3</sup> in size) was placed in 2.5% glutaraldehyde and prefixed overnight at 4°C. It was rinsed three times with 0.1-M PBS and post-fixed by soaking in 1% osmium acid for 2 h. After

rinsing three times with 0.1-M PBS, the tissue was dehydrated step by step in ethanol and then embedded in epoxy resin. Ultrathin sections were prepared at 80 nm, and stained with uranyl acetate and lead citrate. The mitochondrial morphology of acinar cells was observed by transmission electron microscopy (H7000; Hitachi, Tokyo, Japan).

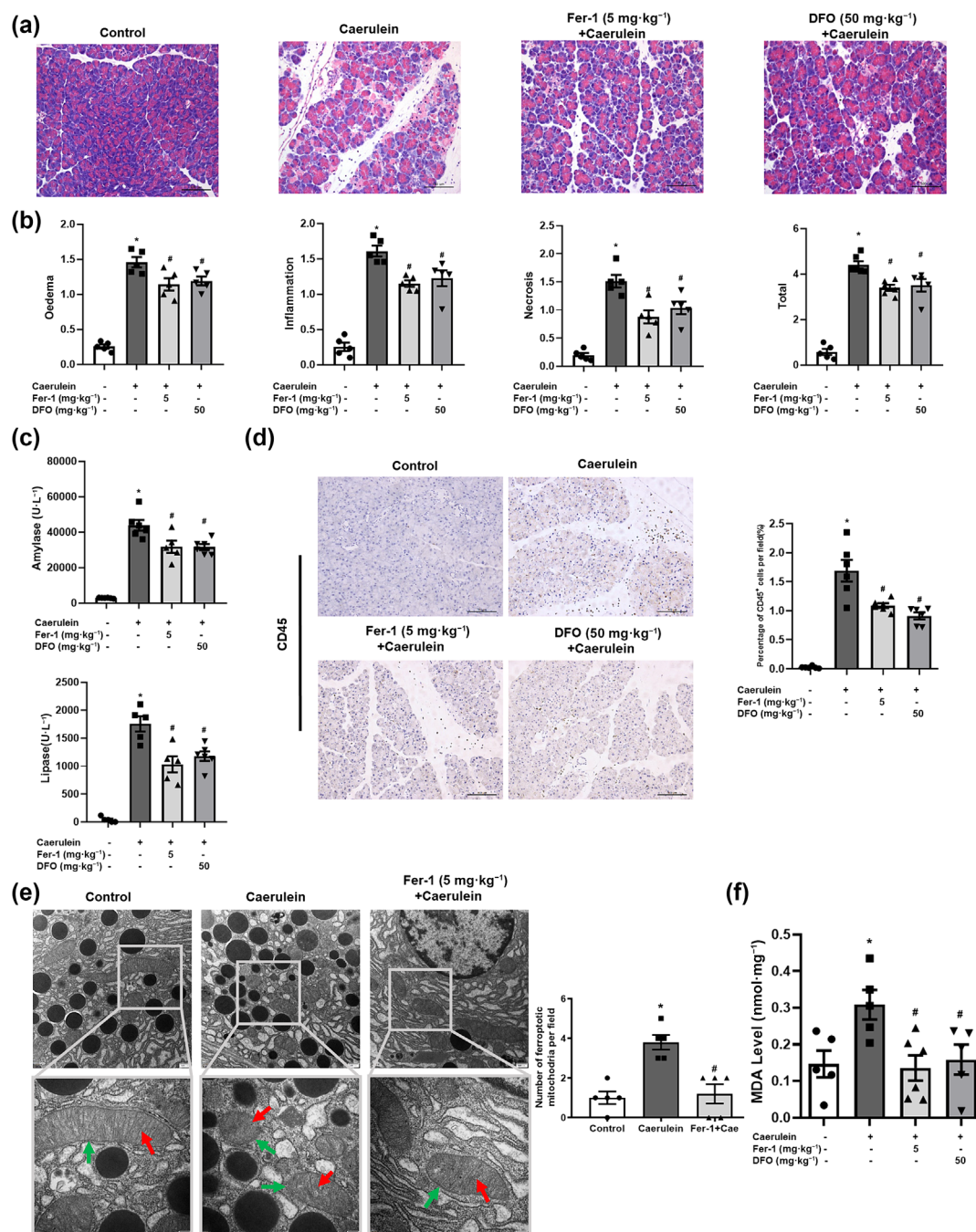


**FIGURE 2** Inhibition of ferroptosis attenuates mitochondrial damage and lipid peroxidation in caerulein induced pancreatitis. Ferostatin-1 (Fer-1, 5 mg·kg<sup>-1</sup>) or deferoxamine mesylate (DFO, 50 mg·kg<sup>-1</sup>) was used 1 h before the first caerulein injection. (a) Representative images of H&E stained pancreatic tissue. Scale bar = 100 μm. (b) Histological scores were determined as described in Section 2. (c) Serum amylase and lipase levels of mice. (d) Immunohistochemical staining of CD45<sup>+</sup> leukocytes in pancreatic tissue. Scale bar = 100 μm. (e) Mitochondrial morphological changes in the acinar cells at low power (scale bar = 500 nm) and high power (scale bar = 200 nm). (f) Pancreatic level of MDA in pancreatic tissues. n = 5 or 6 per group. Data are shown as mean ± SEM. \*P < 0.05 versus control, #P < 0.05 versus Caerulein.

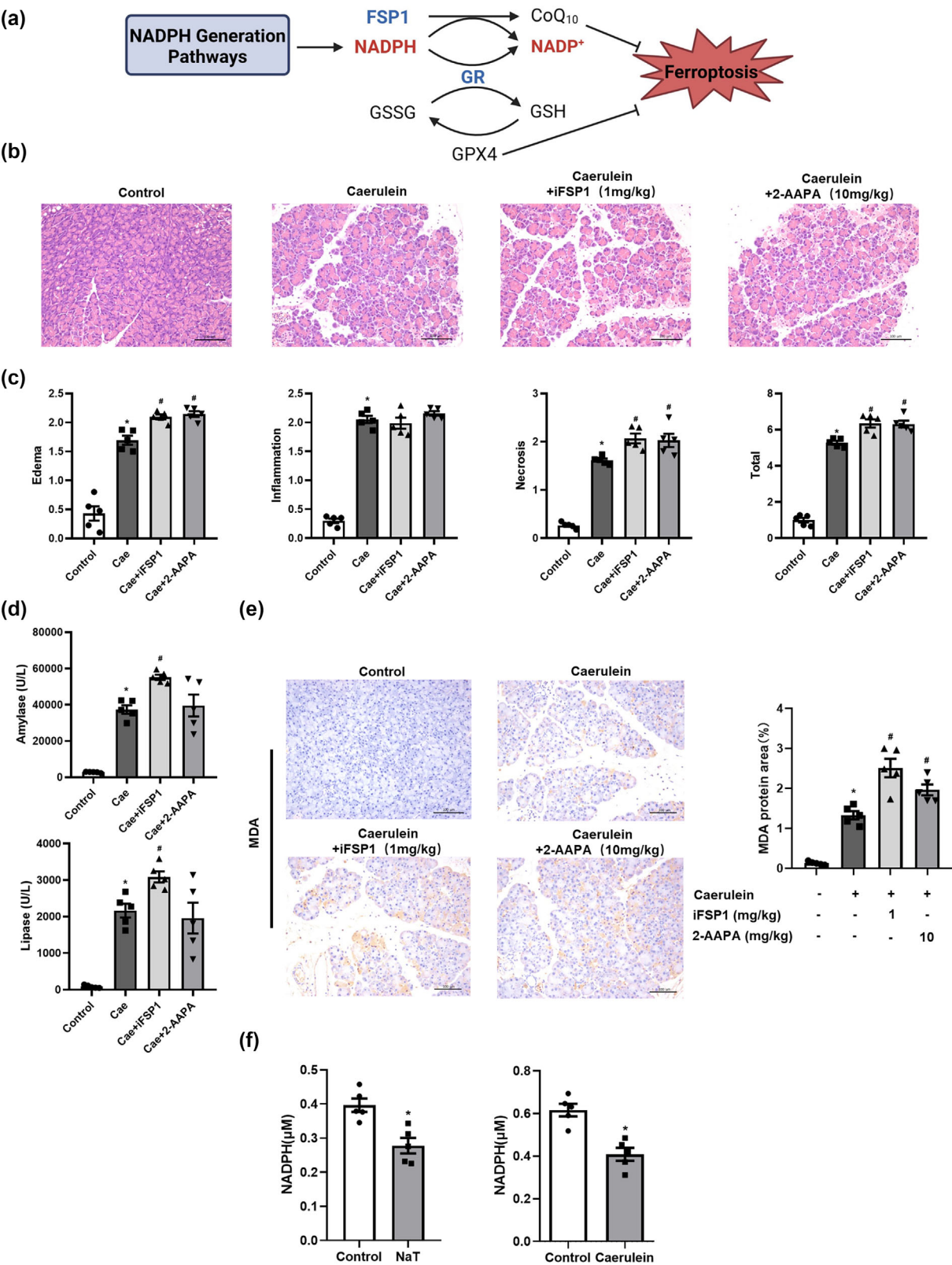


FIGURE 3 Legend on next page.



**FIGURE 3** NADPH-dependent GSH/GPX4 and FSP1/CoQ10 pathways are involved in pancreatic damage in experimental pancreatitis. In vivo, iFSP1 (1 mg·kg<sup>-1</sup>) or 2-AAPA (10 mg·kg<sup>-1</sup>) was used 1 h before the first caerulein injection. In vitro, isolated PACs were pretreated with Fer-1 (5 μM), iFSP1 (5 μM) for 1 h or 2-AAPA (25 μM) for 0.5 h and then stimulated with NaT (4 mM). (a) Schematic diagram depicting the key steps in the regulation of ferroptosis inhibitory pathway. (b) Representative images of H&E stained pancreatic tissue. Scale bar = 100 μm. (c) Histological scores were calculated as described in Section 2. (d) Serum amylase and lipase levels of mice. (e) Immunohistochemical staining of MDA in pancreatic tissue. Scale bar = 100 μm. (f) Levels of NADPH in pancreatic acinar cells (PACs) stimulated by NaT and pancreatic tissues in caerulein-induced acute pancreatitis (AP). n = 5 per group. Data are shown as mean ± SEM. \*P < 0.05 versus control, #P < 0.05 versus Caerulein (Cae), N.S. = not significant.

## 2.16 | Data and statistical analysis

The data and statistical analysis comply with the recommendations on experimental design and analysis in pharmacology (Curtis et al., 2022). Data were presented as mean ± SEM. Comparisons between groups were determined by Student's t-test or one-way ANOVA with Bonferroni's posttest. Bonferroni's posttests were performed only when *F* achieved *P* < 0.05, and there was no significant variance inhomogeneity. Statistical analysis was performed using GraphPad Prism version 8.0 (RRID:SCR\_002798, GraphPad, La Jolla, CA, USA). *P* < 0.05 was considered statistically significant.

## 2.17 | Materials

Caerulein (Cae; cat#HY-A0190), deferoxamine mesylate (cat#HY-B0988), corn oil (cat#HY-Y1888), iFSP1 (cat#HY-136057) and AGI-6780 (AGI; cat#HY-15734) were purchased from Med-ChemExpress (Shanghai, China). Sodium taurocholate hydrate (NaT; cat#86339), tamoxifen (cat#T5648), ferostatin-1 (cat#SML0583), 2-AAPA (cat#A4111) and CoQ<sub>10</sub> (cat#C9538) were from Sigma-Aldrich Chemical (St. Louis, MO, USA). Antibody against amylase (cat# sc-46657, RRID:AB\_626668) was purchased from Santa Cruz Biotechnology (Santa Cruz, CA, USA). Antibodies against Glutathione Peroxidase 4 (GPX4; cat# ab125066, RRID:AB\_10973901), ACSL4 (cat# ab155282, RRID:AB\_2714020), malondialdehyde (MDA; cat#ab243066), IDH2 (cat# ab131263, RRID:AB\_11156098) and FLAG (cat# ab205606, RRID:AB\_2916341) were from Abcam (Cambridge, MA, USA). Antibody against beta-Actin (cat# T0022, RRID:AB\_2839417) was purchased from Affinity Biosciences (OH, USA). Antibody against CD45 (cat# 70257, RRID:AB\_2799780) was purchased from Cell Signaling Technology (Danvers, MA, USA).

## 2.18 | Nomenclature of targets and ligands

Key protein targets and ligands in this article are hyperlinked to corresponding entries in the IUPHAR/BPS Guide to PHARMACOLOGY <http://www.guidetopharmacology.org> and are permanently archived in the Concise Guide to PHARMACOLOGY 2023/23 (Alexander, et al., 2023)

## 3 | RESULTS

### 3.1 | Acinar cell ferroptosis contributes to pancreatic injury in experimental pancreatitis

Emerging studies have implicated ferroptosis in the pathogenesis of AP (Fan et al., 2021; Ma et al., 2021). To investigate whether ferroptosis was present in acinar cells, we detected biochemical signatures of ferroptosis in experimental pancreatitis. The abundance and localization of polyunsaturated fatty acids (PUFAs) determine the degree of intracellular lipid peroxidation, and hence the extent to which ferroptosis is operative (Stockwell et al., 2017). Nontargeted metabolomics showed that the content of PUFAs, such as adrenic acid, arachidonic acid and linoleic acid, was markedly increased in acinar cells upon NaT stimulation (Figure 1a). KEGG pathway analysis demonstrated changes in the biosynthesis of unsaturated fatty acids and the TCA cycle (Figure 1b). Furthermore, in caerulein-induced AP, there was a significant down-regulation of GPX4, a central regulator of the ferroptosis defence system and a concomitant up-regulation of the acyl-coA synthetase long chain family member 4 (ACSL4), an essential component for ferroptosis, compared with the control group (Figure 1c,d). In addition, transmission electron microscopy analysis showed that mice stimulated with caerulein exhibited distinct morphological changes characteristic of ferroptotic cells, including mitochondrial shrinkage, membrane wrinkling and cristae loss (Figure 1e). Quantitative assessments of pancreatic MDA, an end product of lipid peroxidation, further confirmed that lipid peroxidation was significantly elevated in caerulein-induced pancreatitis (Figure 1f). These findings lent support to the hypothesis that ferroptosis is actively involved in the pathophysiology of pancreatic acinar cells during AP.

To clarify the role of acinar cell ferroptosis in AP, we utilized two distinct experimental models: a chemically induced model using caerulein and a clinically relevant model by retrograde infusion of NaT. Prior to AP induction, mice were pretreated with ferroptosis inhibitors, specifically Fer-1 or DFO. Pathological evaluation, including assessments of pancreatic tissue oedema, inflammatory cell infiltration and acinar cell necrosis indicated that inhibition of ferroptosis mitigated the severity of AP in both models (Figure 2a,b, Figure S1A,B). Moreover, Fer-1 or DFO pretreatment markedly decreased serum amylase and lipase levels in caerulein-induced AP although no significant difference was observed in NaT-induced AP, which may be due to the pathological severity and serum biochemical indicators not being exactly parallel in NaT-induced AP (Figure 2c, Figure S1C). Immunohistochemical

staining further revealed that Fer-1 or DFO pretreatment led to a significant reduction in the infiltration of CD45<sup>+</sup> leukocytes into the pancreatic tissues when compared with the AP control group (Figure 2d, Figure S1D). Additionally, ultrastructural analyses using transmission electron microscopy, along with MDA assays, demonstrated that Fer-1 or DFO pretreatment attenuated ferroptotic mitochondrial changes and lipid peroxidation (Figure 2e,f, Figure S1E,F). In addition, there were also changes in the expression of genes related to mitochondrial morphology (Figure S2A,B). Collectively, these findings systematically suggested that ferroptosis played a pivotal role in mediating pancreatic acinar cell injury during AP.

### 3.2 | NADPH-dependent GSH/GPX4 and FSP1/CoQ<sub>10</sub> pathways are involved in pancreatic damage in experimental pancreatitis

Iron-dependent lipid peroxidation serves as the primary mechanism for ferroptosis execution, and the enhancement of lipid peroxide

clearance offers a protective effect against this form of cell death (J. Zheng & Conrad, 2020). As is well known, the primary antioxidant pathways, specifically the GSH/GPX4 and FSP1/CoQ<sub>10</sub> pathways, are pivotal in mitigating ferroptosis by neutralizing lipid peroxides, and these pathways are fuelled by NADPH (Figure 3a). **Glutathione reductase** (GR), an oxidoreductase, facilitates the conversion of oxidized glutathione (GSSG) to its reduced form (GSH) by utilizing NADPH as a cofactor (NaveenKumar et al., 2020). To assess the role of these pathways in acinar cell ferroptosis in AP, mice or PACs were pretreated with the selective inhibitors for FSP1 (iFSP1) or GR (2-AAPA) prior to AP induction. Both iFSP1 and 2-AAPA treatments significantly exacerbated the severity of pancreatitis, as evidenced by histological scoring (Figure 3b,c). Nevertheless, only iFSP1 treatment led to elevated serum levels of amylase and lipase during AP (Figure 3d). Immunohistochemical staining of MDA confirmed that both iFSP1 and 2-AAPA treatments intensified acinar cell lipid peroxidation when compared with the AP group (Figure 3e). In vitro experiments further supported these findings, showing that both iFSP1 and 2-AAPA exacerbated NaT-induced acinar cell injury and

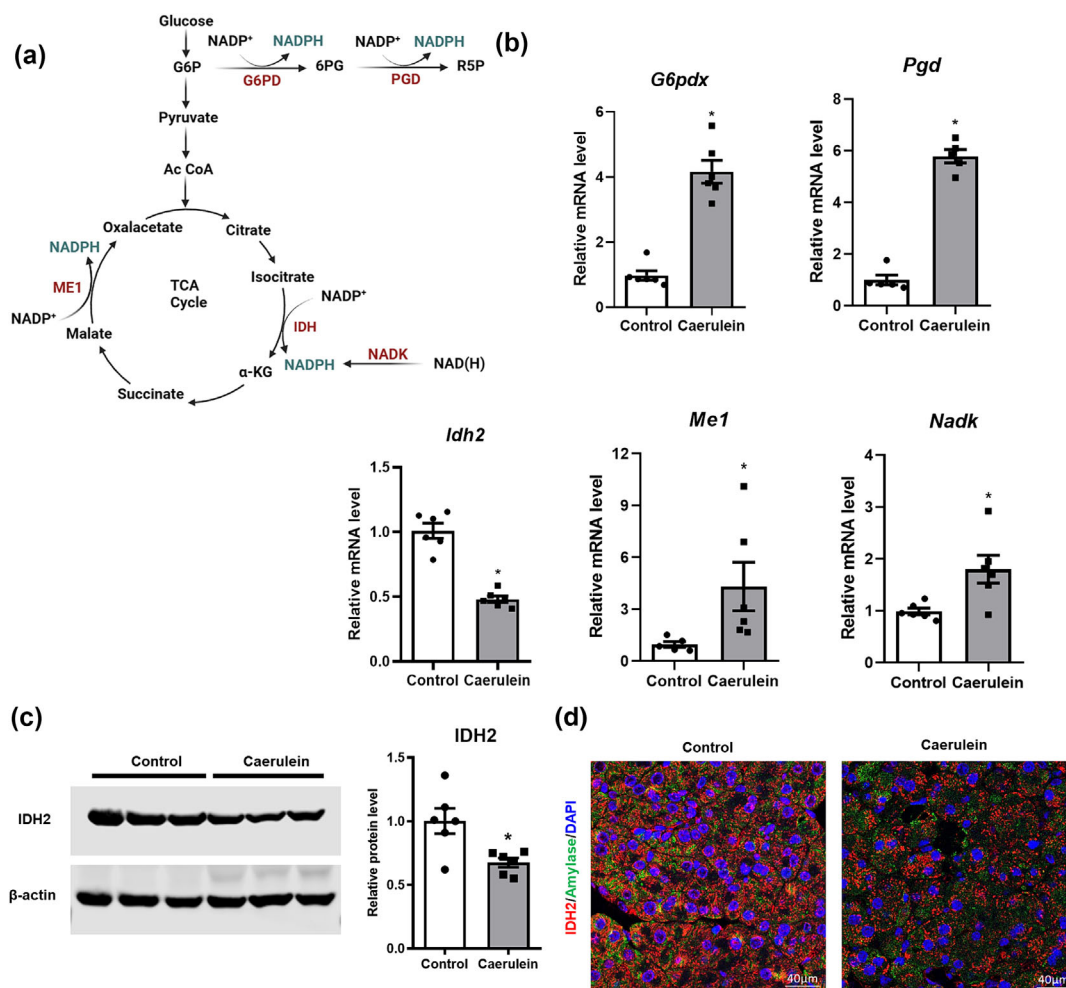


**FIGURE 4** NADPH<sup>+</sup>-dependent isocitrate dehydrogenase 2 (IDH2) is markedly suppressed in experimental pancreatitis. (a,b) Targeted genes regulating NADPH production were analysed in the pancreatic tissues of caerulein induced acute pancreatitis (AP) mice. (c) Representative western blot analysis of IDH2 expression in pancreatic tissue. (d) Immunofluorescence staining of IDH2 and amylase in pancreatic tissue. Nuclei were stained with DAPI. Scale bar = 40 μm. n = 6 per group. Data are shown as mean ± SEM. \*P < 0.05 versus control.



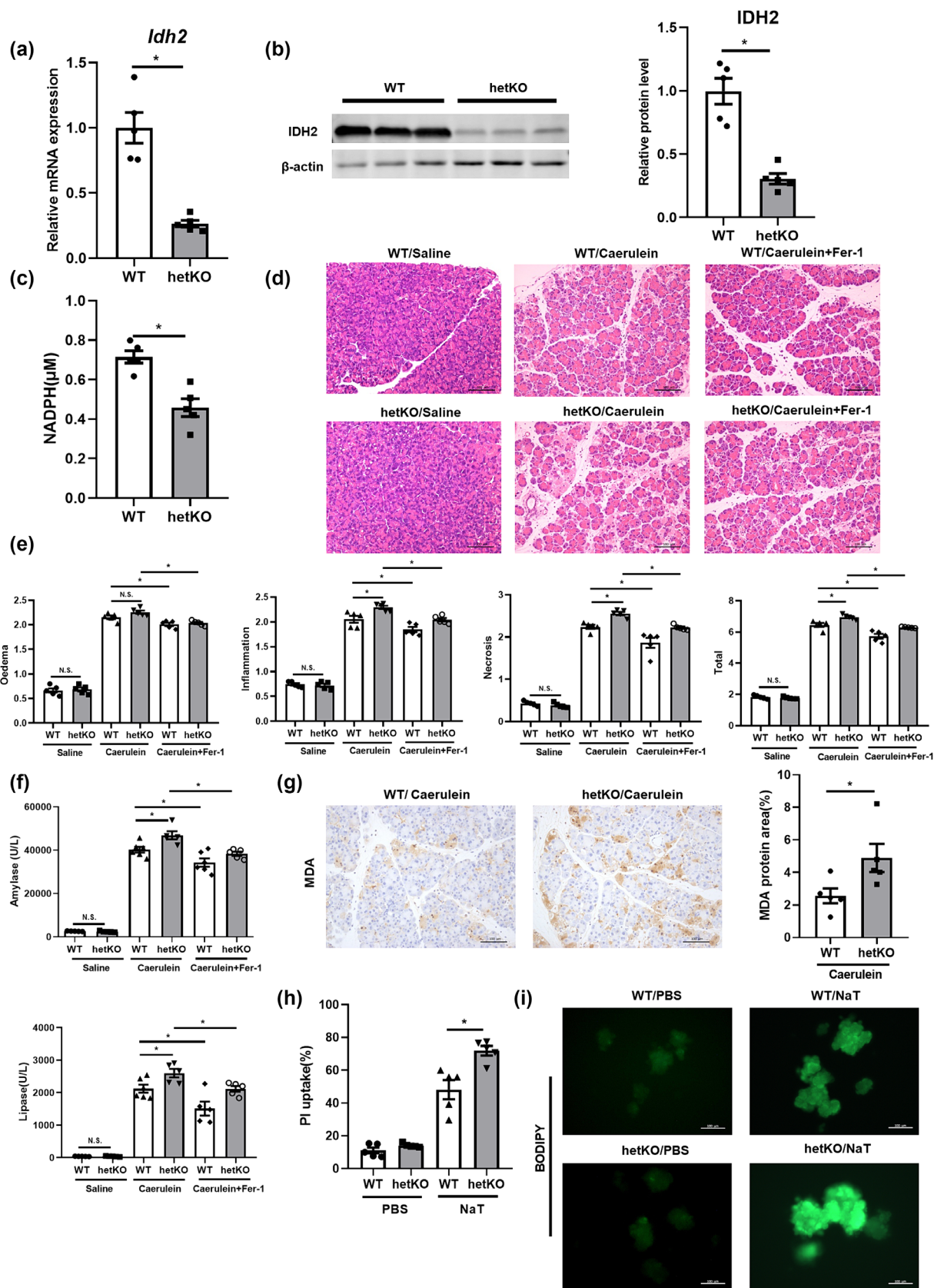


**FIGURE 5** Legend on next page.

**FIGURE 5** Acinar cell-specific deletion of isocitrate dehydrogenase 2 (IDH2) facilitates ferroptosis and exacerbates the severity of experimental pancreatitis. In vivo, Fer-1 ( $5 \text{ mg} \cdot \text{kg}^{-1}$ ) was used 1 h before the first caerulein injection. qRT-PCR (a) and western blot (b) analysis of IDH2 expression in pancreatic acinar cells (PACs) of acinar cell-specific IDH2 knockout mice. (c) The content of NADPH in pancreatic tissue of Ptf1a<sup>CreERT2/-</sup>IDH2<sup>fl/fl</sup> (WT) and Ptf1a<sup>CreERT2/+</sup>IDH2<sup>fl/fl</sup> (hetKO) mice. (d) Representative images of H&E stained pancreatic tissue. Scale bar = 100  $\mu\text{m}$ . (e) Histological scores were analysed as described in Section 2. (f) Serum amylase and lipase of mice. (g) Immunohistochemical staining of MDA in pancreatic tissue. Scale bar = 100  $\mu\text{m}$ . (h) Cell injuries of PACs measured by PI uptake. (i) BODIPY 581/591 staining of PACs in AP. Scale bar = 100  $\mu\text{m}$ .  $n = 5$  or 6 per group. Data are shown as mean  $\pm$  SEM. \* $P < 0.05$ , N.S. = not significant.

lipid peroxidation, effects that were reversible by Fer-1 in vitro (Figure S3A,B). We further measured changes in NADPH levels in the context of AP and found a significant reduction in NADPH levels in both NaT-stimulated acinar cells and pancreatic tissues of caerulein-induced AP mice (Figure 3f). Thus, these data indicated that GSH/GPX4 and FSP1/CoQ<sub>10</sub> pathways acted as suppressors of acinar cell ferroptosis during AP, in which NADPH may serve as a key modulator.

### 3.3 | NADP<sup>+</sup>-dependent isocitrate dehydrogenase (IDH2) is markedly suppressed in experimental pancreatitis

Given the critical role of NADPH in both GSH/GPX4 and FSP1/CoQ<sub>10</sub> pathways, we then examined the genes associated with NADPH metabolism. As is well known, NADPH can be generated through multiple pathways, including the pentose phosphate (PPP) pathway, TCA cycle and NAD kinase (NADK)-catalysed phosphorylation of nicotinamide adenine dinucleotide (NADH) (Figure 4a). According to our data, among these critical enzymes of the NADPH-related pathways, only IDH2 showed significant down-regulation in AP (Figure 4b). IDH2, which is located in the mitochondria, is a pivotal enzyme in the TCA cycle that catalyses the oxidative decarboxylation of isocitrate to produce  $\alpha$ -ketoglutarate ( $\alpha$ -KG) and NADPH (Han et al., 2018). Western blot and immunofluorescence analysis further confirmed the down-regulation of IDH2 in the pancreatic tissues and acinar cells of mice with AP, respectively (Figure 4c,d). Taken together, these findings indicated that NADP<sup>+</sup>-dependent IDH2 was suppressed during AP, potentially impairing lipid peroxide clearance and thereby facilitating acinar cell ferroptosis.

### 3.4 | Acinar cell-specific deletion of isocitrate dehydrogenase (IDH2) facilitates ferroptosis and exacerbates the severity of experimental pancreatitis

To explore the functional significance of IDH2 in modulating acinar cell ferroptosis and the associated-pancreatic injury in AP, we engineered mice harbouring a conditional knockout of IDH2 specifically in pancreatic acinar cells (Ptf1a<sup>CreERT2/+</sup>IDH2<sup>fl/fl</sup>). qPCR and western blot analysis verified an approximately 70% reduction in pancreatic IDH2 expression in these conditional heterozygous knockout (hetKO) mice compared with their wild-type littermates (Figure 5a,b). Moreover, a concomitant decrease of NADPH level was observed in

pancreatic tissues of hetKO mice (Figure 5c). Upon induction of AP using caerulein, the conditional knockout mice manifested exacerbated pancreatic damage, as assessed by elevated histological scoring and serum levels of amylase and lipase compared with control mice (Figure 5d–f). MDA assays showed that IDH2 deficiency led to increased lipid peroxidation in the context of AP (Figure 5g). Notably, treatment with the ferroptosis inhibitor Fer-1 alleviated the exacerbation of pancreatic injury induced by IDH2 deletion (Figure 5d–f). In vitro experiments further supported these findings. PI is a cytosolic fluorescent dye that stains the nucleus by penetrating broken cell membranes and BODIPY 581/591, a ratiometric fluorescent probe, exhibits a red-to-green emission shift in response to lipid peroxidation. PACs with IDH2 deletion exhibited increased injury and lipid peroxidation upon stimulation with NaT, as indicated by an increased percentage of PI uptake and enhanced BODIPY 581/591 staining (Figure 5h,i). Moreover, to further verify the role of IDH2, we pre-treated PACs with the inhibitor of IDH2 (AGI) before AP induction. Notably, AGI-6780 was designed to inhibit mutant IDH2 but was also recently found to inhibit wild-type IDH2 (Jaccard et al., 2023). Our data demonstrated that AGI significantly exacerbated NaT-induced acinar cell injury and lipid peroxidation (Figure S4A,B). Taken together, these data underscored the pivotal role of IDH2 in modulating pancreatic acinar cell ferroptosis and mitigating pancreatic injury during AP.

### 3.5 | The protective effect of isocitrate dehydrogenase (IDH2) overexpression on ferroptosis is involved in the GSH/GPX4 and FSP1/CoQ<sub>10</sub> pathways

Recent research has established the critical roles of GSH/GPX4 and FSP1/CoQ<sub>10</sub> pathways in mitigating ferroptosis, with NADPH serving as an essential cofactor for providing reducing equivalents (Doll et al., 2019; Ursini & Maiorino, 2020). Based on our earlier findings that IDH2 modulated acinar cell ferroptosis and that the IDH2-NADPH pathway was compromised during AP, we hypothesized that the IDH2-NADPH pathway could regulate ferroptosis via the GSH/GPX4 and FSP1/CoQ<sub>10</sub> pathways. IDH2 overexpressing adenovirus was constructed for infection of PACs, which resulted in an approximate 2.5-fold increase in IDH2 expression compared with the Ad-Con group (Figure 6a). We found that adenoviral overexpression of IDH2 led to elevated NADPH levels in PACs (Figure 6b). Furthermore, IDH2 overexpression significantly attenuated NaT-induced acinar cell injury and lipid peroxidation (Figure 6c,d). To discern whether IDH2 exerted its protective effects through the GSH/GPX4

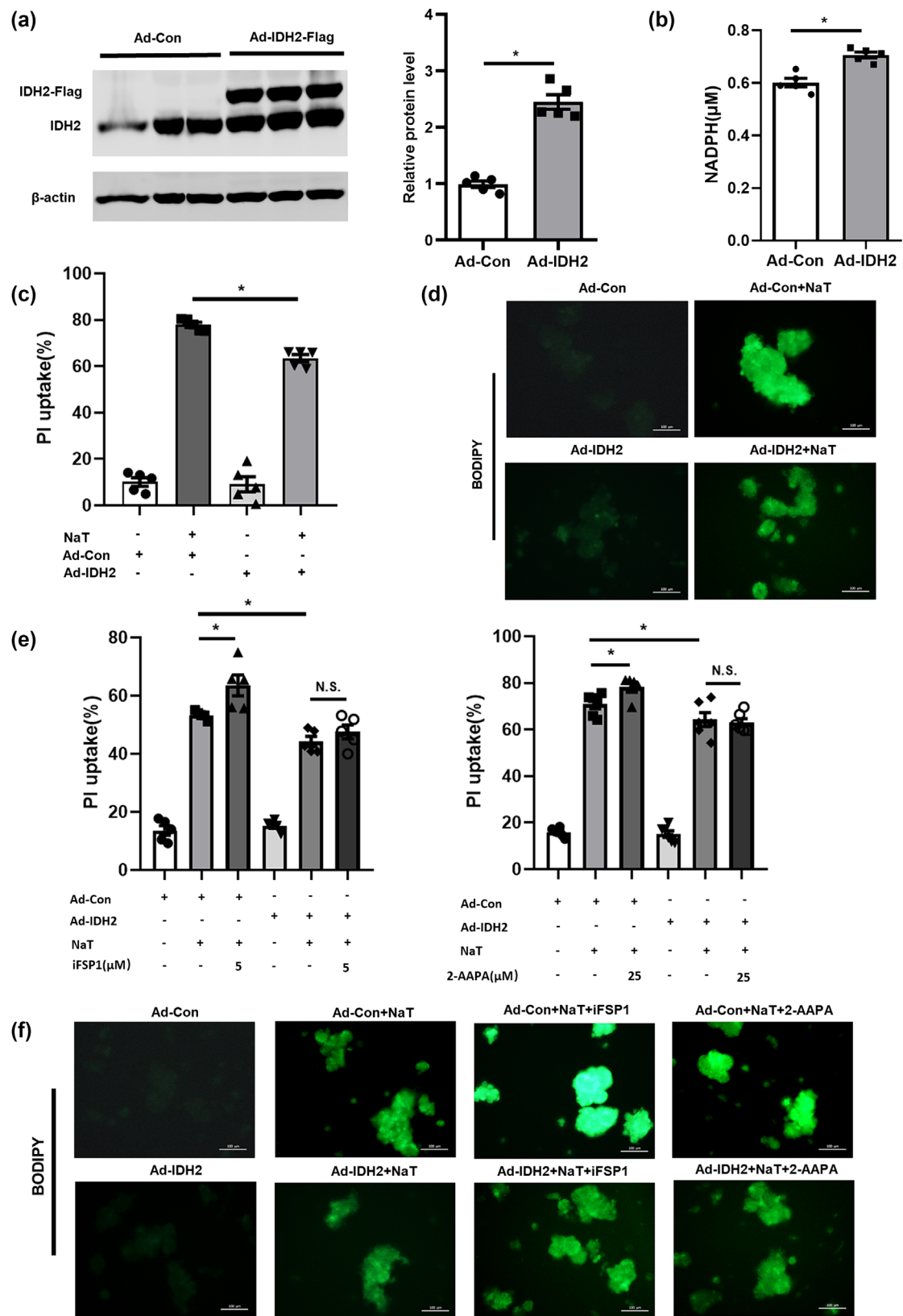


FIGURE 6 Legend on next page.

**FIGURE 6** The protective effect of isocitrate dehydrogenase 2 (IDH2) overexpression on ferroptosis is involved in the GSH/GPX4 and FSP1/CoQ<sub>10</sub> pathways. Isolated pancreatic acinar cells (PACs) with adenovirus-IDH2 (Ad-IDH2) or adenovirus-Con (Ad-Con) were stimulated with sodium taurocholate (NaT) (4 mM). (a) Western blot analysis of IDH2 and IDH2-Flag expression in acinar cells with Ad-IDH2 or Ad-Con. (b) The level of NADPH in acinar cells with Ad-IDH2 or Ad-Con. (c) Cell injuries of PACs measured by PI uptake. (d) BODIPY 581/591 staining of PACs with Ad-IDH2 and Ad-Con stimulated by NaT. Scale bar = 100  $\mu$ m. Isolated PACs with Ad-IDH2 or Ad-Con were pretreated with iFSP1 (5  $\mu$ M) for 1 h or 2-AAPA (25  $\mu$ M) for 0.5 h and then stimulated with NaT (4 mM). (e) Cell injuries of PACs measured by PI uptake. (f) BODIPY 581/591 staining of PACs. Scale bar = 100  $\mu$ m. n = 5 per group. Data are shown as mean  $\pm$  SEM. \**P* < 0.05, N.S. = not significant.

and FSP1/CoQ<sub>10</sub> pathways, we pretreated IDH2-overexpressing acinar cells with either iFSP1 or 2-AAPA prior to NaT stimulation. Both PI uptake and BODIPY 581/591 staining suggested that inhibition of FSP1 or GR negated the protective effects of IDH2 overexpression on acinar cell damage and lipid peroxidation (Figure 6e,f). Collectively, these results identified the IDH2-NADPH circuit as a central signalling hub supporting GSH/GPX4 and FSP1/CoQ<sub>10</sub> pathway to restrict acinar cell ferroptosis and pancreatic injury in the context of AP.

### 3.6 | CoQ<sub>10</sub> supplementation protects against acinar cell ferroptosis and experimental pancreatitis

FSP1, by utilizing NADPH, catalysed the regeneration of reduced CoQ<sub>10</sub>, which in turn inhibits lipid peroxidation and ferroptosis in a GPX4-independent manner (Bersuker et al., 2019). To assess the protective potential of CoQ<sub>10</sub> against pancreatic injury and ferroptosis during AP, CoQ<sub>10</sub> was administered as a pretreatment in both hetKO and control mice. Histopathological analyses revealed a significant attenuation of pancreatic injury in CoQ<sub>10</sub> pretreated mice, as evidenced by improved histological scores (Figure 7a,b). Additionally, serum levels of amylase and lipase were also substantially decreased in the CoQ<sub>10</sub> pretreated group compared with the AP group (Figure 7c). Immunohistochemical staining further corroborated these findings, showing a marked reduction in CD45<sup>+</sup> leukocytes infiltration and lipid peroxidation in both hetKO and control mice following CoQ<sub>10</sub> supplementation (Figure 7d,e). In summary, these data indicated that CoQ<sub>10</sub> supplementation offered a protective effect against experimental pancreatitis via inhibiting acinar cell ferroptosis, thereby presenting a potential therapeutic avenue for clinical AP.

## 4 | DISCUSSION

Approximately 20% of patients with AP progress to more severe disease, typically characterized by necrosis and inflammation-induced systemic damage (Garg & Singh, 2019). Recent studies have demonstrated that ferroptosis, a nonapoptotic form of cell death, is involved in the pathogenesis of AP (H. Li et al., 2022). Nevertheless, the exact molecular mechanisms that control acinar cell ferroptosis is incompletely defined. Here, from the perspective of lipid peroxidation scavenging, our findings revealed the effects of the GSH/GPX4 pathway and the FSP1/CoQ<sub>10</sub> pathway in experimental pancreatitis, in which NADPH played a key role as a reducing equivalent. Furthermore, IDH2, the key enzyme of the TCA cycle, regulated the abundance of

NADPH and acted as a protective agent in AP via NADPH-dependent GSH/GPX4 pathway and FSP1/CoQ<sub>10</sub> pathway (Figure 8).

Ferroptosis is a form of regulatory necrosis, triggered by a combination of iron toxicity, lipid peroxidation and plasma membrane damage, and manipulating the synthesis or degradation processes of PUFAs will ultimately affect the cell susceptibility to ferroptosis (Chen et al., 2021; J. Zheng & Conrad, 2020). The pathogenesis of AP is closely associated with lipid peroxidation and reactive oxygen species (H. Li et al., 2022). Extracellular trypsin increases the susceptibility of acinar cells to ferroptosis by inducing the degradation of glutathione peroxidase 4 (GPX4) through the proteasome 26S subunit, nonadenosine triphosphatase 4-dependent pathway (Liu et al., 2022). High-iron diets or GPX4 depletion accelerates the progression of experimental pancreatitis via oxidative damage (Dai et al., 2020). GPX4 may play a central role in suppressing ferroptosis in the context of AP. Our study systematically addressed the presence of ferroptosis in AP, and revealed that pharmacological inhibition of glutathione reductase, a key enzyme related to the regeneration of reduced GSH in the GSH/GPX4 pathway, could exacerbate the severity of AP, which may result in functional impairment of GPX4. Additionally, inhibition of FSP1, another key enzyme independent of the GPX4-related pathway, likewise exacerbated the severity of AP by interfering with CoQ<sub>10</sub> regeneration. Additionally, significant alterations in the biosynthesis of unsaturated fatty acids were also observed in acinar cells during AP, suggesting that underlying conditions may also exist in AP that induce ferroptosis.

Ferroptosis is governed by antioxidant axes, including the GSH/GPX4 axis and the FSP1/CoQ<sub>10</sub> axis, all of which are fuelled by NADPH (J. Zheng & Conrad, 2020). Research has revealed that NADPH levels were considered as a biomarker of ferroptosis, which negatively correlates with cellular sensitivity to ferroptosis in various cancer cell lines (Shimada et al., 2016). Deficiency of the reducing power of NADPH has been observed during hepatic I/R injury, and NADP<sup>+</sup>-dependent malic enzyme 1 was identified as an anti-ferroptotic regulator by restoring NADPH and GSH levels (Fang et al., 2023). It has been reported that NADPH levels in acinar cells significantly decreased in response to AP stimuli, including ethanol, palmitoleic acid and sodium taurocholate, which is consistent with our data (Booth et al., 2011; Huang et al., 2014). Thus, we suspected that NADPH may play an important role in controlling acinar cell ferroptosis during AP. Notably, NADPH also serves as the substrate for NADPH oxidase (NOX), which causes the production of reactive oxygen species, and inhibition of NOX may block ferroptosis in some diseases (Poursaitidis et al., 2017). Because several studies have indicated that NOX primarily operates in neutrophils rather than acinar cells, we speculated that this condition is not paralleled to acinar cell ferroptosis (Booth et al., 2011; Gukovskaya et al., 2002).



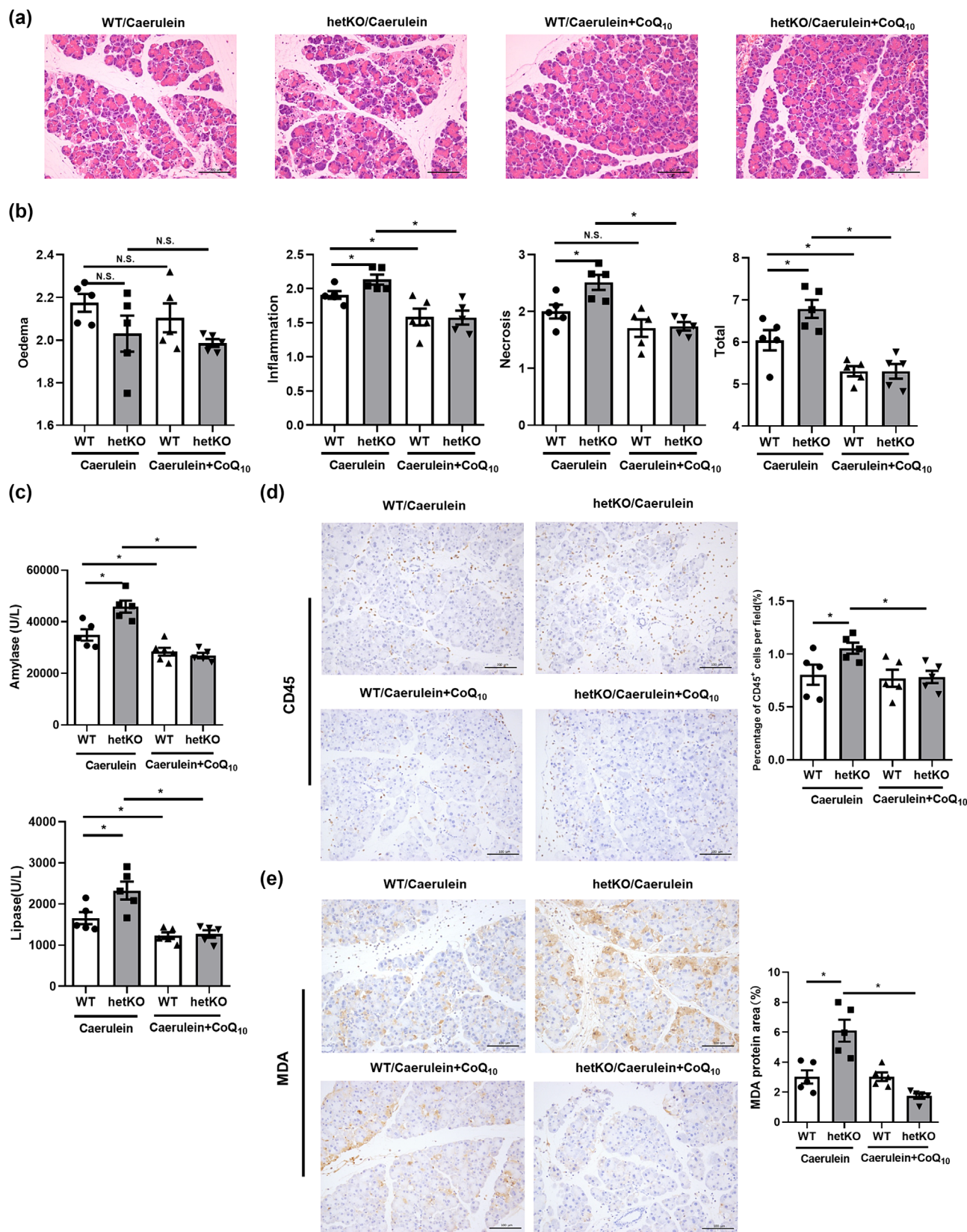
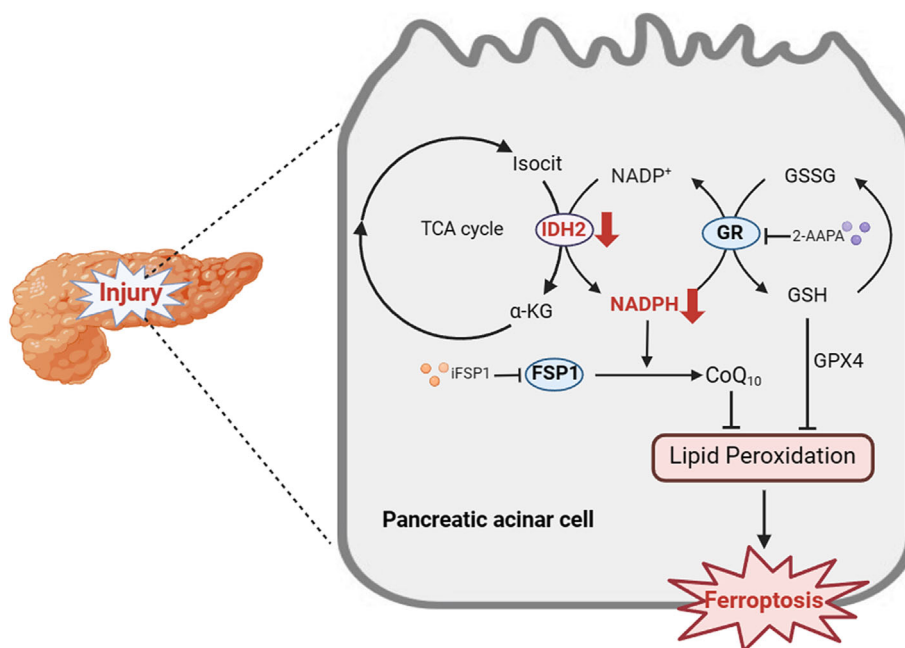


**FIGURE 7** Coenzyme Q<sub>10</sub> (CoQ<sub>10</sub>) supplementation protects against acinar cell ferroptosis and experimental pancreatitis. CoQ<sub>10</sub> (50 mg·kg<sup>-1</sup>) was used 1 h before the first caerulein injection. (a) Representative images of H&E stained pancreatic tissue. Scale bar = 100 μm. (b) Histological scores were analysed as described in Section 2. (c) Serum amylase and lipase levels of mice. (d) Immunohistochemical staining of CD45<sup>+</sup> leucocytes in pancreatic tissue. Scale bar = 100 μm. (e) Immunohistochemical staining of MDA in pancreatic tissue. Scale bar = 100 μm. n = 5 per group. Data are shown as mean ± SEM. \*P < 0.05.



**FIGURE 8** Working model depicting how IDH2-NADPH pathway is regulated and suppresses ferroptosis during AP. IDH2 maintains redox homeostasis by providing reducing equivalents NADPH to the NADPH-dependent GSH/GPX4 pathway and the FSP1/CoQ<sub>10</sub> pathway, thus acting as a protective factor against ferroptosis during AP.



In mammalian cells, the NADPH pool is predominantly generated by several routes, such as the PPP pathway, NADK-catalysed phosphorylation of NADH, NADP<sup>+</sup>-dependent isocitrate dehydrogenase (IDH) and NADP<sup>+</sup>-dependent ME (Fang et al., 2023; Pollak et al., 2007; Zhang et al., 2021). IDH and ME are key enzymes in the TCA cycle. Among them, only mitochondrial IDH2 was markedly decreased in experimental pancreatitis, consistent with the reduction of NADPH, while the PPP pathway, the NADK pathway and the ME pathway were enhanced. This may represent a feedback protective mechanism in acinar cells in response to oxidative stress stimuli. IDH2 located in the mitochondria converts isocitrate to  $\alpha$ -KG by utilizing NADP<sup>+</sup> as a co-factor, and its mutants are extensively described in tumour initiation and progression (Dang et al., 2016). IDH2 maintains a pool of reduced glutathione and peroxiredoxin by furnishing mitochondrial NADPH to NADPH-dependent antioxidant enzymes, including glutathione reductase and thioredoxin reductase (Tommasini-Ghelfi et al., 2019). In kidney ischaemia-reperfusion injury, IDH2 knockdown impaired the reduction of NADP<sup>+</sup> and GSSG in mitochondria, exacerbating mitochondrial structural and functional damage (Han et al., 2017). Moreover, studies have suggested that IDH2 deregulation in HT1080 fibrosarcoma and Hepa1-6 hepatoma cells increases sensitivity to ferroptosis (Kim et al., 2020). Our current study demonstrated that modulation of IDH2 expression affected pancreatic injury upon AP by impacting NADPH availability in acinar cells. In particular, the protective effect of adenoviral overexpression of IDH2 on acinar cell injury could be mitigated by the inhibition of FSP1 and GR, suggesting that the effect of the IDH2-NADPH pathway on pancreatic injury depended on the GSH/GPX4 pathway and the FSP1/CoQ<sub>10</sub> pathway.

CoQ<sub>10</sub>, the downstream molecule in the FSP1/CoQ<sub>10</sub> pathway, is a fat-soluble benzoquinone-like vitamin and the third most commonly consumed dietary supplement with a favourable safety profile (Arenas-Jal et al., 2020). The fully reduced form of CoQ<sub>10</sub> is a

lipophilic antioxidant with the ability to neutralize free radicals and regenerate vitamin E in its reduced state. Studies have shown that the exogenous supplementation of CoQ<sub>10</sub> was found to significantly attenuate experimental pancreatitis, while the exact mechanism was unclear (Mirmalek et al., 2016; Shin et al., 2020). Our findings indicated that CoQ<sub>10</sub> supplementation inhibited lipid peroxidation in pancreatic tissues, thereby alleviating the severity of AP, suggesting that CoQ<sub>10</sub> could be a promising therapeutic strategy for treating acute pancreatitis. More broadly, this research could provide a preclinical theoretical basis for purposing of the IDH2-NADPH pathway and its downstream targets into clinical trials for AP treatment.

Nevertheless, we cannot exclude other mechanisms involved in IDH2-regulated acinar cell injury. Deletion of IDH2 during ischaemia-reperfusion disrupts the balance between mitochondrial fusion and fission, leading to higher fragmentation (Han et al., 2017). Because mitochondrial dysfunction mediates significant pathological responses of AP (Biczko et al., 2018), IDH2 could be involved in pancreatic injury by affecting mitochondrial function and thus pancreatic injury.  $\alpha$ -KG, another product of IDH2, regulates both anabolic and catabolic products of the TCA cycle, thereby controlling amino acid synthesis and ATP production. It may also be involved in pancreatic injury during AP (Zdzisinska et al., 2017).

In summary, the IDH2-NADPH pathway could be a protective factor against ferroptosis and pancreatic injury. Unravelling the complex metabolic regulation of oxidative damage and the underlying mechanisms of ferroptosis in AP may be pivotal in guiding the development of severe AP therapies.

#### AUTHOR CONTRIBUTIONS

G. Hu, X. Han and J. Ni designed and conceived the study. G. Hu and B. Li provided funding to support the study. Q. Peng, B. Li and P. Song performed the experiments, collected and analysed the data. R. Wang, J. Jiang, X. Jin, J. Shen and J. Bao provided technical support in the

in vivo and in vitro experiments. Q. Peng and B. Li drafted the manuscript. G. Hu, X. Han and J. Ni supervised the study and revised the manuscript. All the authors approved the final version of the manuscript.

## ACKNOWLEDGEMENTS

The authors thank Professor Jing Xue from Institute of State Key Laboratory of Oncogenes and Related Genes, Stem Cell Research Center, Ren Ji Hospital, Shanghai Jiao Tong University School of Medicine, Shanghai, China, for providing Ptf1a<sup>CreERT2</sup> mice. This work was sponsored by National Natural Science Foundation of China to G.H. (8217031247 and 81970556) and B.L. (82200716).

## CONFLICT OF INTEREST STATEMENT

The authors declare no conflicts of interest.

## DATA AVAILABILITY STATEMENT

N/A-Review.

## DECLARATION OF TRANSPARENCY AND SCIENTIFIC RIGOUR

This Declaration acknowledges that this paper adheres to the principles for transparent reporting and scientific rigour of preclinical research as stated in the *BJP* guidelines for [Design & Analysis](#), [Immunoblotting and Immunochemistry](#) and [Animal Experimentation](#) and as recommended by funding agencies, publishers and other organizations engaged with supporting research.

## ORCID

Jianbo Ni  <https://orcid.org/0000-0002-1219-9083>

Guoyong Hu  <https://orcid.org/0000-0003-3550-6127>

## REFERENCES

- Alexander, S. P. H., Fabbro, D., Kelly, E., Mathie, A. A., Peters, J. A., Veale, E. L., Armstrong, J. F., Faccenda, E., Harding, S. D., Davies, J. A., Annett, S., Boison, D., Burns, K. E., Dessauer, C., Gertsch, J., Helsby, N. A., Izzo, A. A., Ostrom, R., Papapetropoulos, A., ... Wong, S. S. (2023). The Concise Guide to PHARMACOLOGY 2023/24: Enzymes. *British Journal of Pharmacology*, 180, S289–S373. <https://doi.org/10.1111/bph.16181>
- Alexander, S. P. H., Roberts, R. E., Broughton, B. R. S., Sobey, C. G., George, C. H., Stanford, S. C., Cirino, G., Docherty, J. R., Gienbycz, M. A., Hoyer, D., Insel, P. A., Izzo, A. A., Ji, Y., MacEwan, D. J., Mangum, J., Wonnacott, S., & Ahluwalia, A. (2018). Goals and practicalities of immunoblotting and immunohistochemistry: A guide for submission to the British Journal of Pharmacology. *British Journal of Pharmacology*, 175(3), 407–411. <https://doi.org/10.1111/bph.14112>
- Arenas-Jal, M., Sune-Negre, J. M., & Garcia-Montoya, E. (2020). Coenzyme Q10 supplementation: Efficacy, safety, and formulation challenges. *Comprehensive Reviews in Food Science and Food Safety*, 19(2), 574–594. <https://doi.org/10.1111/1541-4337.12539>
- Bersuker, K., Hendricks, J. M., Li, Z., Magtanong, L., Ford, B., Tang, P. H., Roberts, M. A., Tong, B., Maimone, T. J., Zoncu, R., Bassik, M. C., Nomura, D. K., Dixon, S. J., & Olzmann, J. A. (2019). The CoQ oxidoreductase FSP1 acts parallel to GPX4 to inhibit ferroptosis. *Nature*, 575(7784), 688–692. <https://doi.org/10.1038/s41586-019-1705-2>
- Biczko, G., Vegh, E. T., Shalbueva, N., Mareninova, O. A., Elperin, J., Lotshaw, E., Gretler, S., Lugea, A., Malla, S. R., Dawson, D., Ruchala, P., Whitelegge, J., French, S. W., Wen, L., Husain, S. Z., Gorelick, F. S., Hegyi, P., Rakonczay, Z. Jr., Gukovsky, I., & Gukovskaya, A. S. (2018). Mitochondrial dysfunction, through impaired autophagy, leads to endoplasmic reticulum stress, deregulated lipid metabolism, and pancreatitis in animal models. *Gastroenterology*, 154(3), 689–703. <https://doi.org/10.1053/j.gastro.2017.10.012>
- Booth, D. M., Murphy, J. A., Mukherjee, R., Awais, M., Neoptolemos, J. P., Gerasimenko, O. V., Tepikin, A. V., Petersen, O. H., Sutton, R., & Criddle, D. N. (2011). Reactive oxygen species induced by bile acid induce apoptosis and protect against necrosis in pancreatic acinar cells. *Gastroenterology*, 140(7), 2116–2125. <https://doi.org/10.1053/j.gastro.2011.02.054>
- Chen, X., Kang, R., Kroemer, G., & Tang, D. (2021). Ferroptosis in infection, inflammation, and immunity. *The Journal of Experimental Medicine*, 218(6), e20210518. <https://doi.org/10.1084/jem.20210518>
- Curtis, M. J., Alexander, S. P. H., Cirino, G., George, C. H., Kendall, D. A., Insel, P. A., Izzo, A. A., Ji, Y., Panettieri, R. A., Patel, H. H., Sobey, C. G., Stanford, S. C., Stanley, P., Stefanska, B., Stephens, G. J., Teixeira, M. M., Vergnolle, N., & Ahluwalia, A. (2022). Planning experiments: Updated guidance on experimental design and analysis and their reporting III. *British Journal of Pharmacology*, 179(15), 3907–3913. <https://doi.org/10.1111/bph.15868>
- Dai, E., Han, L., Liu, J., Xie, Y., Zeh, H. J., Kang, R., Bai, L., & Tang, D. (2020). Ferroptotic damage promotes pancreatic tumorigenesis through a TMEM173/STING-dependent DNA sensor pathway. *Nature Communications*, 11(1), 6339. <https://doi.org/10.1038/s41467-020-20154-8>
- Dang, L., Yen, K., & Attar, E. C. (2016). IDH mutations in cancer and progress toward development of targeted therapeutics. *Annals of Oncology*, 27(4), 599–608. <https://doi.org/10.1093/annonc/mdw013>
- Ding, C. C., Rose, J., Sun, T., Wu, J., Chen, P. H., Lin, C. C., Yang, W. H., Chen, K. Y., Lee, H., Xu, E., Tian, S., Akinwuntan, J., Zhao, J., Guan, Z., Zhou, P., & Chi, J. T. (2020). MESH1 is a cytosolic NADPH phosphatase that regulates ferroptosis. *Nature Metabolism*, 2(3), 270–277. <https://doi.org/10.1038/s42255-020-0181-1>
- Dixon, S. J., Lemberg, K. M., Lamprecht, M. R., Skouta, R., Zaitsev, E. M., Gleason, C. E., Patel, D. N., Bauer, A. J., Cantley, A. M., Yang, W. S., Morrison, B. 3rd, Stockwell, B. R., & Stockwell, B. R. (2012). Ferroptosis: An iron-dependent form of nonapoptotic cell death. *Cell*, 149(5), 1060–1072. <https://doi.org/10.1016/j.cell.2012.03.042>
- Doll, S., Freitas, F. P., Shah, R., Aldrovandi, M., da Silva, M. C., Ingold, I., Goya Grocin, A., Xavier da Silva, T. N., Panzilius, E., Scheel, C. H., Mourão, A., Buday, K., Sato, M., Wanninger, J., Vignane, T., Mohana, V., Rehberg, M., Flatley, A., Schepers, A., ... Conrad, M. (2019). FSP1 is a glutathione-independent ferroptosis suppressor. *Nature*, 575(7784), 693–698. <https://doi.org/10.1038/s41586-019-1707-0>
- Fan, R., Sui, J., Dong, X., Jing, B., & Gao, Z. (2021). Wedelolactone alleviates acute pancreatitis and associated lung injury via GPX4 mediated suppression of pyroptosis and ferroptosis. *Free Radical Biology & Medicine*, 173, 29–40. <https://doi.org/10.1016/j.freeradbiomed.2021.07.009>
- Fang, X., Zhang, J., Li, Y., Song, Y., Yu, Y., Cai, Z., Lian, F., Yang, J., Min, J., & Wang, F. (2023). Malic enzyme 1 as a novel anti-Ferroptotic regulator in hepatic ischemia/reperfusion injury. *Advanced Science (Weinh)*, 10(13), e2205436. <https://doi.org/10.1002/adv.202205436>
- Friedmann Angeli, J. P., Schneider, M., Proneth, B., Tyurina, Y. Y., Tyurin, V. A., Hammond, V. J., Herbach, N., Aichler, M., Walch, A., Eggenhofer, E., Basavarajappa, D., Rådmark, O., Kobayashi, S., Seibt, T., Beck, H., Neff, F., Esposito, I., Wanke, R., Förster, H., ... Conrad, M. (2014). Inactivation of the ferroptosis regulator Gpx4 triggers acute renal failure in mice. *Nature Cell Biology*, 16(12), 1180–1191. <https://doi.org/10.1038/ncb3064>

- Garg, P. K., & Singh, V. P. (2019). Organ failure due to systemic injury in acute pancreatitis. *Gastroenterology*, 156(7), 2008–2023. <https://doi.org/10.1053/j.gastro.2018.12.041>
- Gukovskaya, A. S., Vaquero, E., Zaninovic, V., Gorelick, F. S., Lusi, A. J., Brennan, M. L., Holland, S., & Pandol, S. J. (2002). Neutrophils and NADPH oxidase mediate intrapancreatic trypsin activation in murine experimental acute pancreatitis. *Gastroenterology*, 122(4), 974–984. <https://doi.org/10.1053/gast.2002.32409>
- Han, S. J., Choi, H. S., Kim, J. I., Park, J. W., & Park, K. M. (2018). IDH2 deficiency increases the liver susceptibility to ischemia-reperfusion injury via increased mitochondrial oxidative injury. *Redox Biology*, 14, 142–153. <https://doi.org/10.1016/j.redox.2017.09.003>
- Han, S. J., Jang, H. S., Noh, M. R., Kim, J., Kong, M. J., Kim, J. I., Park, J. W., & Park, K. M. (2017). Mitochondrial NADP(+)-dependent isocitrate dehydrogenase deficiency exacerbates mitochondrial and cell damage after kidney ischemia-reperfusion injury. *Journal of the American Society of Nephrology*, 28(4), 1200–1215. <https://doi.org/10.1681/ASN.2016030349>
- Hu, G., Shen, J., Cheng, L., Guo, C., Xu, X., Wang, F., Huang, L., Yang, L., He, M., Xiang, D., Zhu, S., Wu, M., Yu, Y., Han, W., & Wang, X. (2011). Reg4 protects against acinar cell necrosis in experimental pancreatitis. *Gut*, 60(6), 820–828. <https://doi.org/10.1136/gut.2010.215178>
- Huang, W., Booth, D. M., Cane, M. C., Chvanov, M., Javed, M. A., Elliott, V. L., Armstrong, J. A., Dingsdale, H., Cash, N., Li, Y., Greenhalf, W., Mukherjee, R., Kaphalia, B. S., Jaffar, M., Petersen, O. H., Tepikin, A. V., Sutton, R., & Criddle, D. N. (2014). Fatty acid ethyl ester synthase inhibition ameliorates ethanol-induced Ca<sup>2+</sup>-dependent mitochondrial dysfunction and acute pancreatitis. *Gut*, 63(8), 1313–1324. <https://doi.org/10.1136/gutjnl-2012-304058>
- Jaccard, A., Wyss, T., Maldonado-Perez, N., Rath, J. A., Bevilacqua, A., Peng, J. J., Lepez, A., Von Gunten, C., Franco, F., Kao, K. C., Camviel, N., Martín, F., Ghesquière, B., Migliorini, D., Arber, C., Romero, P., Ho, P. C., & Wenes, M. (2023). Reductive carboxylation epigenetically instructs T cell differentiation. *Nature*, 621(7980), 849–856. <https://doi.org/10.1038/s41586-023-06546-y>
- Kim, H., Lee, J. H., & Park, J. W. (2020). Down-regulation of IDH2 sensitizes cancer cells to erastin-induced ferroptosis. *Biochemical and Biophysical Research Communications*, 525(2), 366–371. <https://doi.org/10.1016/j.bbrc.2020.02.093>
- Lee, P. J., & Papachristou, G. I. (2019). New insights into acute pancreatitis. *Nature Reviews. Gastroenterology & Hepatology*, 16(8), 479–496. <https://doi.org/10.1038/s41575-019-0158-2>
- Li, B., Wu, J., Bao, J., Han, X., Shen, S., Ye, X., Dai, J., Wu, Z., Niu, M., He, Y., Ni, J., Wen, L., Wang, X., & Hu, G. (2020). Activation of alpha7-nACh receptor protects against acute pancreatitis through enhancing TFEB-regulated autophagy. *Biochimica et Biophysica Acta - Molecular Basis of Disease*, 1866(12), 165971. <https://doi.org/10.1016/j.bbdis.2020.165971>
- Li, H., Lin, Y., Zhang, L., Zhao, J., & Li, P. (2022). Ferroptosis and its emerging roles in acute pancreatitis. *Chinese Medical Journal*, 135(17), 2026–2034. <https://doi.org/10.1097/CM9.0000000000002096>
- Lilley, E., Stanford, S. C., Kendall, D. E., Alexander, S. P. H., Cirino, G., Docherty, J. R., George, C. H., Insel, P. A., Izzo, A. A., Ji, Y., Panettieri, R. A., Sobey, C. G., Stefanska, B., Stephens, G., Teixeira, M., & Ahluwalia, A. (2020). ARRIVE 2.0 and the British Journal of Pharmacology: Updated guidance for 2020. *British Journal of Pharmacology*, 177(16), 3611–3616. <https://doi.org/10.1111/bph.15178>
- Liu, K., Liu, J., Zou, B., Li, C., Zeh, H. J., Kang, R., Kroemer, G., Huang, J., & Tang, D. (2022). Trypsin-mediated sensitization to Ferroptosis increases the severity of pancreatitis in mice. *Cellular and Molecular Gastroenterology and Hepatology*, 13(2), 483–500. <https://doi.org/10.1016/j.jcmgh.2021.09.008>
- Ma, D., Li, C., Jiang, P., Jiang, Y., Wang, J., & Zhang, D. (2021). Inhibition of ferroptosis attenuates acute kidney injury in rats with severe acute pancreatitis. *Digestive Diseases and Sciences*, 66(2), 483–492. <https://doi.org/10.1007/s10620-020-06225-2>
- Mederos, M. A., Reber, H. A., & Girgis, M. D. (2021). Acute pancreatitis: A review. *JAMA*, 325(4), 382–390. <https://doi.org/10.1001/jama.2020.20317>
- Mirmalek, S. A., Gholamrezaei Boushehrinejad, A., Yavari, H., Kardeh, B., Parsa, Y., Salimi-Tabatabaee, S. A., Yadollah-Damavandi, S., Parsa, T., Shahverdi, E., & Jangholi, E. (2016). Antioxidant and anti-inflammatory effects of coenzyme Q10 on L-arginine-induced acute pancreatitis in rat. *Oxidative Medicine and Cellular Longevity*, 2016, 5818479. <https://doi.org/10.1155/2016/5818479>
- NaveenKumar, S. K., Hemshekhar, M., Jagadish, S., Manikanta, K., Vishalakshi, G. J., Kemparaju, K., & Girish, K. S. (2020). Melatonin restores neutrophil functions and prevents apoptosis amid dysfunctional glutathione redox system. *Journal of Pineal Research*, 69(3), e12676. <https://doi.org/10.1111/jpi.12676>
- Percie du Sert, N., Hurst, V., Ahluwalia, A., Alam, S., Avey, M. T., Baker, M., Browne, W. J., Clark, A., Cuthill, I. C., Dirnagl, U., Emerson, M., Garner, P., Holgate, S. T., Howells, D. W., Karp, N. A., Lazic, S. E., Lidster, K., MacCallum, C. J., Macleod, M., ... Wurbel, H. (2020). The ARRIVE guidelines 2.0: Updated guidelines for reporting animal research. *PLoS Biology*, 18(7), e3000410. <https://doi.org/10.1371/journal.pbio.3000410>
- Perides, G., van Acker, G. J., Laukkanen, J. M., & Steer, M. L. (2010). Experimental acute biliary pancreatitis induced by retrograde infusion of bile acids into the mouse pancreatic duct. *Nature Protocols*, 5(2), 335–341. <https://doi.org/10.1038/nprot.2009.243>
- Pollak, N., Dolle, C., & Ziegler, M. (2007). The power to reduce: Pyridine nucleotides--small molecules with a multitude of functions. *The Biochemical Journal*, 402(2), 205–218. <https://doi.org/10.1042/BJ20061638>
- Poursaitidis, I., Wang, X., Crighton, T., Labuschagne, C., Mason, D., Cramer, S. L., Triplett, K., Roy, R., Pardo, O. E., Seckl, M. J., Rowlinson, S. W., Stone, E., & Lamb, R. F. (2017). Oncogene-selective sensitivity to synchronous cell death following modulation of the amino acid nutrient cystine. *Cell Reports*, 18(11), 2547–2556. <https://doi.org/10.1016/j.celrep.2017.02.054>
- Shimada, K., Hayano, M., Pagano, N. C., & Stockwell, B. R. (2016). Cell-line selectivity improves the predictive power of pharmacogenomic analyses and helps identify NADPH as biomarker for ferroptosis sensitivity. *Cell Chemical Biology*, 23(2), 225–235. <https://doi.org/10.1016/j.chembiol.2015.11.016>
- Shin, J. Y., Choi, J. W., Kim, D. G., Zhou, Z. Q., Shin, Y. K., Seo, J. H., Song, H. J., Choi, B. M., Bae, G. S., & Park, S. J. (2020). Protective effects of coenzyme Q10 against acute pancreatitis. *International Immunopharmacology*, 88, 106900. <https://doi.org/10.1016/j.intimp.2020.106900>
- Stockwell, B. R., Friedmann Angeli, J. P., Bayir, H., Bush, A. I., Conrad, M., Dixon, S. J., Fulda, S., Gascón, S., Hatzios, S. K., Kagan, V. E., Noel, K., Jiang, X., Linkermann, A., Murphy, M. E., Overholtzer, M., Oyagi, A., Pagnussat, G. C., Park, J., Ran, Q., ... Zhang, D. D. (2017). Ferroptosis: A regulated cell death nexus linking metabolism, redox biology, and disease. *Cell*, 171(2), 273–285. <https://doi.org/10.1016/j.cell.2017.09.021>
- Tang, D., Chen, X., Kang, R., & Kroemer, G. (2021). Ferroptosis: Molecular mechanisms and health implications. *Cell Research*, 31(2), 107–125. <https://doi.org/10.1038/s41422-020-00441-1>
- Tommasini-Ghelfi, S., Murnan, K., Kouri, F. M., Mahajan, A. S., May, J. L., & Stegh, A. H. J. S. (2019). Cancer-associated mutation and beyond: The emerging biology of isocitrate dehydrogenases in human disease. *Science Advances*, 5(5), eaaw4543. <https://doi.org/10.1126/sciadv.aaw4543>
- Ursini, F., & Maiorino, M. (2020). Lipid peroxidation and ferroptosis: The role of GSH and GPx4. *Free Radical Biology & Medicine*, 152, 175–185. <https://doi.org/10.1016/j.freeradbiomed.2020.02.027>

- Wang, G., Qu, F. Z., Li, L., Lv, J. C., & Sun, B. (2016). Necroptosis: A potential, promising target and switch in acute pancreatitis. *Apoptosis*, 21(2), 121–129. <https://doi.org/10.1007/s10495-015-1192-3>
- Wen, L., Voronina, S., Javed, M. A., Awais, M., Szatmary, P., Latawiec, D., Chvanov, M., Collier, D., Huang, W., Barrett, J., Begg, M., Stauderman, K., Roos, J., Grigoryev, S., Ramos, S., Rogers, E., Whitten, J., Velicelebi, G., Dunn, M., ... Sutton, R. (2015). Inhibitors of ORAI1 prevent cytosolic calcium-associated injury of human pancreatic acinar cells and acute pancreatitis in 3 mouse models. *Gastroenterology*, 149(2), 481–492 e487. <https://doi.org/10.1053/j.gastro.2015.04.015>
- Wildi, S., Kleeff, J., Mayerle, J., Zimmermann, A., Bottinger, E. P., Wakefield, L., Büchler, M. W., Friess, H., & Korc, M. (2007). Suppression of transforming growth factor beta signalling aborts caerulein induced pancreatitis and eliminates restricted stimulation at high caerulein concentrations. *Gut*, 56(5), 685–692. <https://doi.org/10.1136/gut.2006.105833>
- Zdzisinska, B., Zurek, A., & Kandefer-Szerszen, M. (2017). Alpha-ketoglutarate as a molecule with pleiotropic activity: Well-known and novel possibilities of therapeutic use. *Archivum Immunologiae et Therapiae Experimentalis (Warsz)*, 65(1), 21–36. <https://doi.org/10.1007/s00005-016-0406-x>
- Zhang, Y., Xu, Y., Lu, W., Ghergurovich, J. M., Guo, L., Blair, I. A., Rabinowitz, J. D., & Yang, X. (2021). Upregulation of antioxidant capacity and nucleotide precursor availability suffices for oncogenic transformation. *Cell Metabolism*, 33(1), 94–109 e108. <https://doi.org/10.1016/j.cmet.2020.10.002>
- Zheng, J., & Conrad, M. (2020). The metabolic underpinnings of ferroptosis. *Cell Metabolism*, 32(6), 920–937. <https://doi.org/10.1016/j.cmet.2020.10.011>
- Zheng, Y., Sun, W., Shan, C., Li, B., Liu, J., Xing, H., Xu, Q., Cui, B., Zhu, W., Chen, J., Liu, L., Yang, T., Sun, N., & Li, X. (2022). Beta-hydroxybutyrate inhibits ferroptosis-mediated pancreatic damage in acute liver failure through the increase of H3K9bbh. *Cell Reports*, 41(12), 111847. <https://doi.org/10.1016/j.celrep.2022.111847>

## SUPPORTING INFORMATION

Additional supporting information can be found online in the Supporting Information section at the end of this article.

**How to cite this article:** Peng, Q., Li, B., Song, P., Wang, R., Jiang, J., Jin, X., Shen, J., Bao, J., Ni, J., Han, X., & Hu, G. (2024). IDH2-NADPH pathway protects against acute pancreatitis via suppressing acinar cell ferroptosis. *British Journal of Pharmacology*, 1–18. <https://doi.org/10.1111/bph.16469>